

Iterative Computation of Singular and Singularity induced Bifurcation points of Differential Algebraic equations for a Multi-machine Power system Model

Subodh Kumar Mohanty, Sasmita Jena

Gandhi Institute of Excellent Technocrats, Bhubaneswar, India

Vedang Institute of Technology, Khordha, Odisha, India

ABSTRACT—In this paper, we present an efficient algorithm to compute singular points and singularity-induced bifurcation points of differential-algebraic equations for a multi-machine power-system model. Power systems are often modeled as a set of differential-algebraic equations (DAE) whose algebraic part brings singularity issues into dynamic stability assessment of power systems. Roughly speaking, the singular points are points that satisfy the algebraic equations, but at which the vector field is not defined. In terms of power-system dynamics, around singular points, the generator angles (the natural states variables) are not defined as a graph of the load bus variables (the algebraic variables). Thus, the causal requirement of the DAE model breaks down and it cannot predict system behavior. Singular points constitute important organizing elements of power-system DAE models. This paper proposes an iterative method to compute singular points at any given parameter value. With a lemma presented in this paper, we are also able to locate singularity induced bifurcation points upon identifying the singular points.

I. INTRODUCTION

BIFURCATION theory is the commonly used tool to analyze various types of stability problems in power systems modeled either as a set of ordinary differential equations (ODEs) or as a set of differential-algebraic equations (DAEs) [1]. In the former case, the equations are notoriously stiff when certain load dynamics are included. As a modeling tool, problems associated with this affect further analytical studies of the system. In order to overcome this problem (as well as the fact of the nonexistence of a universally accepted dynamical load model) DAEs have been used based on the approximation of these relatively fast and stable load dynamics as algebraic equations [2]–[8].

This paper addresses the local bifurcations and algebraic singularities of the classical power system with a constant PQ load model, which is modeled as semi-explicit index-1 DAEs. It is well known that when parameters are subject to variations, the equilibria of the DAE power-system model may exhibit three local bifurcations, namely saddle node (SN), Hopf, and singularity induced (SI) bifurcations. The SN and Hopf bifurcations, which are observed in the ODE models of power systems as well, have been extensively studied in power systems and they are linked to voltage collapse and oscillatory instabilities,

respectively [1]. The SI bifurcation is due to singularity of the algebraic equations of the DAE model under some parameter variations.

With an SI bifurcation theorem ([7, Th. 3, p. 19–99]), an improved version of it based on the decomposition of parameter dependent polynomials. More recent work on the SI bifurcations includes the [10] and [11]. In [10], Beardmore has extended the SI bifurcation theorem of [7] to include non-generic cases where branching of equilibria is located at the singularity, i.e., [7, Assumption 2, SI bifurcation Theorem] is removed and applied to a 3-bus power system, which has been also studied by Kwatny et al. in [2]. In [11], Riza et al. have provided a detailed study on the qualitative nature of singular points of relatively simple index-1 DAE examples indicating that in some cases dynamic behavior of the system is smooth (well-defined vector field) even at singular points.

An important implication of the occurrence of the SI bifurcation is the existence of a singular set (or an impassable surface) in the constraint manifold containing infinitely many singular points at each parameter value, which may play a crucial role in assessing the stability of DAE power-system models. The literature in power-system stability analysis with respect to the algebraic singularities of the DAEs is rich with references describing voltage instabilities in terms of the following. Nearness to

an impasse surface [12], [13] sudden change in voltages [14], [15] and eventual (or actual) loss of voltage causality [2], [12], to name a few. In [14] the existence of the impasse surface is closely related to the load models, and for constant load model the DAE model has the properties of voltage instability (i.e., sudden reduction in voltages) when operating in the vicinity of impasse points (or trajectories coinciding with the impasse surface).

More related work have reported been with similar results and using the bifurcation theory they have shown that an important part of the stability boundary is formed by trajectories that are tangent to the singular surface. More recent studies [16], [17] focus on the direct assessment of the system stability in the presence of the impasse surface that lies on the stability boundary. A new engineering technique has been presented to compute the critical energy over the relevant segment of the impasse surface that guarantee the causality if the system has less energy than the critical value.

In spite of the fact that there is no well-established link between algebraic singularity and voltage collapse as in the case of the SN bifurcation, most of the works suggest that the system undergoes some sort of voltage instability when the voltage causality is lost during a transient. With respect to loss of voltage causality, it is essential to note that during this, voltages are no longer implicit functions of dynamic variables when described by DAE models. To use DAE as a tool, knowledge of where causality disappears (or where impasse surface(s) "lie") can be applied toward the definition of "limits" of appropriateness for a given model. An underlying issue is that at singular points (including singular equilibria); the DAE model cannot predict the voltage behavior. Thus, location of singularities, which constitute important organizing elements of a power-system DAE model, is invaluable information for assessing stability of the system. The family of singular points forms a boundary of well-defined behavior for a given model. In this work impasse surface is a set of singular points that exhibit loss of voltage causality.

Even though many researchers either in the field of power systems [2], [5]–[8], [12]–[17] or in the field of the general DAE theory [9]–[11] have long recognized the importance of singular points (or loss of voltage causality in power systems) including singular equilibria in terms of system dynamics, there is no rigorous method available in the literature for computing their locations in the parameter space. Most of the effort focuses on characterizing qualitative description of system

dynamics around singularities without providing a systematic method for locating them, especially for larger power systems.

Our main purpose here is to propose a simple and efficient method to identify algebraic singularities (including singular equilibria) of the DAE model of power systems and to visualize singularities together with the equilibria and their associated local bifurcations as a function of the parameters using traditional nose curves. The proposed method involves the following two main steps.

- 1) Computing singular points at various parameter values along the nose curve defined by a designated bus injection change pattern and illustrating singular points in a two-dimensional (2-D) nose curve
- 2) Developing a lemma showing that any singular point at a given set of generator bus injections is also an equilibrium point (thus, it is a SI bifurcation point) at another set of bus injections.

In the method for computing singular points, we first use generator angles to parameterize the algebraic part of the DAE model at any given parameter value (i.e., bus injections) and formulate the problem of identifying singular points as a bifurcation problem of a set of algebraic equations whose parameters

The rest of the paper is organized as follows. Section II discusses bifurcations and singularities of the DAE model of the classical power system. Section II also includes a lemma to identify the SI bifurcations and presents two examples of the DAE (one of which is a 5-bus power-system example) to

illustrate the application of the lemma and the key concept of the paper. Section III describes methods to compute equilibria and singular points of the DAE model in details. Section IV presents the simulation results using voltage stability toolbox (VST) [18], [19] for the IEEE 118-bus system and illustrates singular points in the nose curve. Finally, Section V summarizes main contributions of this work and suggests some of the related future work.

II. DIFFERENTIAL-ALGEBRAIC POWER-SYSTEM MODEL AND SINGULARITIES

A. Classical Power System Model

The dynamics of a classical power system with constant PQ load buses are commonly described by semi-explicit DAE of the form [2]

$$\dot{\omega} = -[M^{-1}D]\omega - M^{-1}[f_g(\delta_g, \delta_\ell, V) - P_g]$$

$$f_\ell(\delta_g, \delta_\ell, V) - P_\ell = 0$$

$$Q_\ell \quad (2.1)$$

where δ_g is the vector of generators' rotor angles, δ_ℓ is the vector of generators' angular velocities, δ_ℓ is the vector of phase angles of voltages at the load buses, V is the vector of voltage magnitudes, P_g is the inertia matrix, D is the damping matrix, P_g is the vector of net real power injections at the generator buses, and finally P_ℓ and Q_ℓ are the vectors of net real and reactive power injections at the load buses, respectively. The differential equation is the swing equation representing generator dynamics, and algebraic equations are the power flow equations at the load buses. In order to obtain a compact form of (2.1), let

$$x = \begin{bmatrix} \delta_g \\ \dot{\delta}_g \\ \delta_\ell \\ V \end{bmatrix}, y = \begin{bmatrix} \beta_g \\ \beta_\ell \end{bmatrix}$$

and $g(x, y) = \begin{bmatrix} f(x, y) - \beta_g \\ Q_\ell \end{bmatrix}$, then, we have

$$\dot{x} = g(x, y) \quad (2.2)$$

where and

For a network consisting of n_g number of generators and n_{pq} number of PQ load buses the parameter vector is in the form of P_g and denotes net real power injection to the number of generators (note that generator bus #1 is chosen as the swing bus of the system). The set of parameters $Q_\ell^T = [P_{n_g+1} \dots P_{n_g+n_{pq}}]^T$ denotes the load demands at the number of load buses where P_{n_g+i} and Q_{n_g+i} are the real and reactive power demands, respectively. For the sake of simplicity in the notation, from this point forward, we assume that $x \in \mathbb{R}^m$, $y \in \mathbb{R}^k$ and $\beta \in \mathbb{R}^l$ where $\beta = [\beta_g^T \beta_\ell^T]^T$.

The DAE model of (2.2) has two essential features: 1) explicit parameter dependence and 2) differential-algebraic structure. The parameter dependence implies that the system equilibria may exhibit local bifurcations when parameters are subject to variation. These bifurcations are SN, Hopf, and SI bifurcations. The SI bifurcation, which is not observed for the ODEs model of power systems, is due to the algebraic structure. The main focus of this paper is singularities of DAE model (2.2) including SI bifurcations. In Section II-B, we briefly describe those bifurcations focusing on

the SI bifurcations.

B. Local Bifurcations and Singularities of the DAE Power System Model

Local bifurcations of the equilibria associated with the changes of the parameter β have been observed in the DAE model of power systems. Various types of bifurcations and associated computational issues are summarized in [5] and [7]. The first step to analyze bifurcations is to compute various equilibria when the parameter β is varied. For a given set of β this parameter, an equilibrium point satisfies two sets of algebraic equations. This set of all equilibrium points is defined as follows:

$$g(x, y) = 0 \quad (2.3)$$

The stability of the DAE systems is more complicated than for systems described by ODEs due to algebraic structure of the model. The algebraic part of (2.2) requires that any motion be constrained to the set $M = \{(x, y) \in \mathbb{R}^m \times \mathbb{R}^k \mid g(x, y) = 0\}$. The vector field may not be well defined at all points of M . At any point $(x, y) \in M$, we have $J = \begin{bmatrix} D_x g(x, y) \\ D_y g(x, y) - \beta_\ell \end{bmatrix}$ and if J is nonsingular, then is uniquely defined by $\dot{x} = -J^{-1} [D_y g(x, y) - \beta_\ell]$.

If J is singular at a point (x, y) , then the vector field is not well defined at that point. Typically, such singular points lie on codimension 1 submanifolds of M .

Definition [5]: Suppose M is a regular manifold for all $(x, y) \in M$, and that $[D_y g(x, y) - \beta_\ell] \neq 0$. Then (x^*, y^*) is said to be causal (x^*, y^*, β^*) . Otherwise, it is noncausal.

The causality of a point could be extended to the causality of a region as follows [14], [15]:

$$C_p(\beta) = \{(x, y) \in M \mid \det [D_y g(x, y) - \beta_\ell] \neq 0; [D_y g(x, y) - \beta_\ell] \text{ has negative real eigenvalues}\} \quad (2.7)$$

The region C_p is called a voltage causal region or solutions sheet [13] and is the voltage causal region index. Within any voltage causal region, load bus voltages and angles follow generator angles' behavior. At any causal point in the region, the implicit function theorem ensures that there exists a function $\psi(x, \beta) = \psi(x^*, \beta)$ defined on a neighborhood of (x^*, β) such that $g(x, \psi(x, \beta)) - \beta_\ell = 0$ with y^* and that satisfies

It follows that within a voltage causal region, trajectories of the DAE are locally defined by the ODEs (2.8)

Typically, in a major part of the constraint manifold, such

reduction is possible and the ODEs uniquely define the dynamic behavior of DAEs. However, the constraint manifold will, in general, contain noncasual points (or singular points) at which equivalence is not possible. These singular points that lie in the boundary of voltage causal regions form a singular surface (or impasse surface) in the constraint manifold [7],[15]

$$\{(x, y) \in \mathbb{R}^{n+m} \mid g(x, y) - \beta_t = 0, \beta = \text{constant}\} \quad (2.4)$$

Typically, we expect to be composed of one or more dis-connected (differentiable) manifolds [20] called components. In general, when we refer to, we will mean a particular one of these components called the principal component is a regular manifold of dimension m if

$$\text{rank} \begin{bmatrix} \frac{\partial g}{\partial x} & \frac{\partial g}{\partial y} \end{bmatrix} = m \quad \text{on } M. \quad (2.5)$$

The structure of depends, of course, on the parameter β . Even for very simple power-system models, (2.5) may not be satisfied for some values of. The manifold is the state space for the dynamical system defined by (2.2) which induces a vector field

Over casual regions, system dynamic behavior evolves according to a locally equivalent ODE system representation. However, trajectories that encounter the singular surface typically undergo loss of existence/uniqueness. The DAE model breaks down and fails to predict the system behavior.

Local bifurcation analyses of power systems identify qualitative changes in system equilibria of ODE system of (2.8) such as number of equilibria and their stability features as the parameters are subject to vary slowly; and these bifurcation concepts can be easily extended to DAE systems of (2.2) [5]. The stability feature of an equilibrium point

and associated local bifurcations are determined by the eigenvalues of the reduced system matrix if is nonsingular

$$(2.10)$$

$$S(\beta) = \left\{ (x, y) \in \mathbb{R}^{n+m} \mid \begin{array}{l} g(x, y) - \beta_t = 0, \\ \det[D_y(g(x, y) - \beta_t)] \neq 0 \end{array} \right\}$$

$$(x_0, y_0)$$

$$[D_y(g(x, y) - \beta_t)]$$

$$[A_{\text{sys}}] = D_x f|_0 - D_y f|_0 [D_y g|_0]^{-1} D_y g|_0.$$

The SN bifurcation occurs when a stable equilibrium point (SEP), meets a type-1 unstable equilibrium point (UEP), at a parameter value β_{SN} to form an equilibrium point $x_0(\beta_{SN}) = x_0^*(\beta_{SN})$. The corresponding reduced system matrix $[A_r]$ has a simple eigenvalue at the origin, and certain transversality conditions are met [21], [22]. If the parameter β increases beyond the bifurcation value β_{SN} , then, it disappears and there are no other equilibrium points nearby. The consequence of the loss of equilibria is that the system states change dynamically. In particular, dynamics can be such that the system voltages fall in a voltage collapse. The SN bifurcation has become a widely accepted paradigm for one important form of voltage instability and linked to voltage collapse [23], [24]. In an appropriate parameter space such as megawatt (MW) real power transfer, the SN bifurcation point, also known as the maximum loading point or point of collapse, provides information on the static stability margin of the current operating point. Hopf bifurcation occurs when a pair of complex conjugate eigenvalues moves from the left to the right half of the complex plane, or vice versa, crossing the imaginary axis at points other than the origin. The importance of Hopf bifurcation has been increasingly recognized, as it became clear that stability of the equilibrium could be lost by this mechanism well before reaching the point of collapse for the large power systems. Such a detailed analysis of oscillatory instability related to Hopf bifurcation for the disturbance occurred on June 12, 1992, on the Midwestern segment of US interconnections system has been reported in [25] for a DAE model of a real power system. The last local bifurcation of interest is the SI bifurcation that occurs when an equilibrium point, say (x_s, y_s) , encounters the singularity of the algebraic equation at the parameter β_{SI} . The SI bifurcation refers to stability change due to an eigenvalue of the reduced system matrix associated with the equilibrium point diverging to infinity from either to, or vice versa [7]. Similar type of instantaneous change in the eigenvalues of reduced system matrix is also observed in the case of limit induced (LI) bifurcation that occurs when the control limits such as limit on the field voltage are reached [26]. However, in the LI bifurcation case, these changes are small compared to those of SI bifurcation case. The set of SI bifurcations is defined as follows: [27] have proposed a singularly perturbed differential equation (SPDE) as the power system model and their simulation results indicate that a rapid decline in bus voltage magnitudes may occur if trajectories pass close to the singular surface. More

recently, Huang et al. [28] has also used SPDE model to analyze system behavior and through eigenvalue analysis they have shown that the SPDE model will have the same dynamic behavior as the reduced ODEs if some adjustments on the sign of the algebraic equations are made. Note that in the DAE of (2.2), the parameter β_g is decoupled from the rest of the equations, and at the singular points (not singular equilibria) there exists real power mismatches at the generator buses (i.e., $f(x_s, y_s) - \beta_{sg} \neq 0$). This decoupled-parameter structure allows us to locate SI bifurcation point when a singular point, say (x_s, y_s) , belonging to the singular set of (2.9) and the corresponding nonzero real power mismatches at the generator buses are known. The following lemma, which exploits this decoupled structure, shows that it is possible to find a new set of parameters such that (x_s, y_s) will be a singular equilibrium point. Lemma: A singular point of (2.2) (x_s, y_s) at a given parameter value β_{sg} is also an equilibrium point, hence, an SI bifurcation point, at another parameter value β_{sg}^{new} . Proof: Suppose that (x_s, y_s) is a singular point of the decoupled DAE of (2.2) at the parameter value $\beta = \beta_{sg}$ such that
$$\begin{bmatrix} \beta_g^T & \beta_g^T \end{bmatrix}^T \dot{x} = f(x_s, y_s) - \beta_{sg} \neq 0$$

$$0 = g(x_s, y_s) - \beta_{sg}$$
 (2.12)
$$\det[D_y(g(x_s, y_s) - \beta_{sg})] = 0.$$
 Observe that since (x_s, y_s) is not (in general) an equilibrium point, and we have a nonzero mismatch at the generator buses. Let this mismatch be $f(x_s, y_s) - \beta_{sg} \neq 0$. In order to force a zero mismatch at the generator buses, we can always define a new set of injections, $\Delta\beta_{sg}$, at the generator buses such that
$$\dot{x} = f(x_s, y_s) - (\beta_{sg} + \Delta\beta_{sg})$$

$$= f(x_s, y_s) - \beta_{sg}^{new} = 0$$

$$0 = g(x_s, y_s) - \beta_{sg}$$
 (2.13)
$$\det[D_y(g(x_s, y_s) - \beta_{sg})] = 0.$$

$$0 \in \mathbb{R} \Rightarrow 0$$
 (2.11) The singularity of β_{sg} (similarly, β_{sg}^{new}) implies that the system will experience some form of instability problem resulting from fast interaction of network variables. However, it is difficult to predict the nature of instability owing to modeling

surface cutting it. It is worth to state that there is no reason to expect the singular surface to form a smooth surface as shown in Fig. 1. However, we do expect it to be a set (not necessarily) connected with a boundary. This 2-

D singular surface (shown as planar) is really an approximation of a nonplanar surface that will actually cut the 3-D equilibrium surface. Note that a nose curve that shows the evolution of

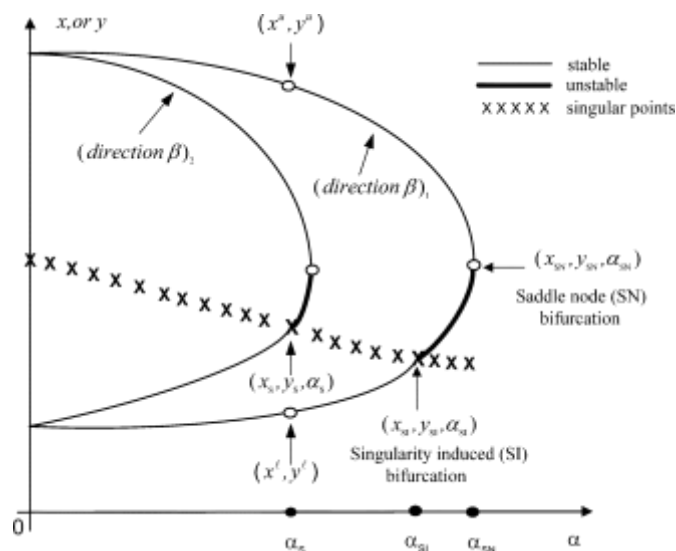


Fig. 2. Illustration of bifurcations of equilibria and singular points in a 2-D nose curve.

the equilibria is plotted for a particular load increase pattern. Two equilibrium points of the nose curve at a given parameter value are also depicted, namely upper and lower voltage solutions, and they are labeled as (x^u, y^u, α) and (x^l, y^l, α) , respectively. This nose curve represents the equilibrium set of (2.3) and dashed surface represents the singular surface given by (2.9). When the nose curve crosses the singular surface, the SI bifurcation occurs. The SI bifurcation point on the surface is labeled by (x^s, y^s, α_s) . It is expected that for different load increase patterns the nose curve will cross the singular surface at different points indicating other SI bifurcations as can be seen in Fig. 2. Fig. 2 shows two nose curves each representing a different bus injection increase pattern defined by $(\text{direction } \beta)_1$ and $(\text{direction } \beta)_2$. Note that along the nose curve of $(\text{direction } \beta)_1$ two local bifurcations, SN, and SI bifurcations and stability characteristics of the equilibria are illustrated schematically. Note that various singular points are denoted by (x) as the bifurcation parameter varies. Our main idea here is to depict stability limits of operating points in the presence of algebraic singularities. The traditional

$$(V^u, \delta^u, \alpha) \quad (V^l, \delta^l, \alpha)$$

α

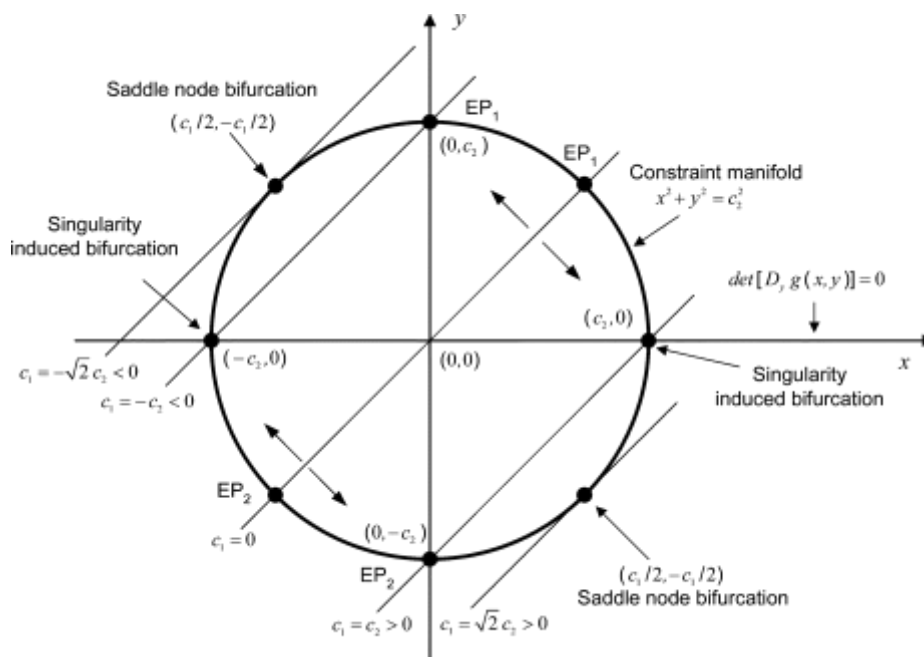


Fig.3. Illustration of SN and SI bifurcations.

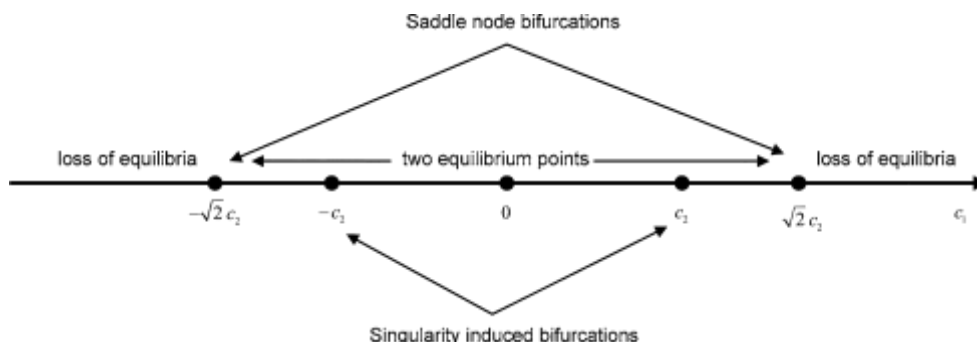


Fig.4. SN and SI bifurcations with qualitative changes in the number of equilibrium points as a function of c_1 and c_2 .

nose curves (or PV curves) are usually used to indicate stability margins imposed by various local bifurcations in the parameter space. We bring singularity information

$$\dot{x} = -x + y + c_1 = f(x, y, c_1)$$

into the nose curve and illustrate changes in both equilibria and singular points as the bifurcation parameter slowly changes. This way of bringing singularity information gathered from the constraint manifold to the parameter space gives a visual representation of both static and dynamic stability boundaries together in the same picture, as shown in Fig. 2.

In Section II-C, we provide two illustrative examples of the DAE model (one of which is a power system example) in order to show the types of bifurcations in the solution structure of the system equilibria, singularities of the constraint manifold, and the application of the lemma.

C. Two Illustrative Examples

Example I: Consider the following parameter-dependent DAE:

$$= x^2 + y^2 \quad (2.16)$$

where x is the dynamic state variable, y is the algebraic variable and, c_1, c_2 are the parameters.

Note that the DAE of (2.16) is in the form of (2.2) where parameters are decoupled from the rest of the equations.

Observe that for any given parameter values, equilibrium points are the intersection of the two curves: 1) a line, and

2) a circle centered at the origin with a radius c_2 . Fig. 3 shows the constraint manifold (i.e., $x^2 + y^2 = c_2^2$) and various equilibria as well as their bifurcations depending on the parameter c_1 .

For $c_1 < 0$, there are two dynamic SEPs labeled as EP_1 and EP_2 for $c_1 < 0$ in Fig. 3. However,

when c_1 is subject to vary in either positive or negative direction, we observe bifurcations of the equilibria. First bifurcation occurs at the parameters

when one of the stable equilibria for increasing in positive direction or decreasing in negative direction coincides with the singularities of the constraint manifold. This is an SN bifurcation.

Observe that the constraint manifold has singularities at $\{(-c_2, 0); (c_2, 0)\}$ for which the Jacobian matrix of the algebraic equation of (2.16) (i.e.,

$[D_y g(x_d, y, c_2)]_{c_1=0}$) has a simple eigenvalue at the origin. Further increase in c_1 causes one of the stable equilibria to cross the singular surface and to become a type-1 UEP. These two

equilibria are shown in Fig. 3. However,

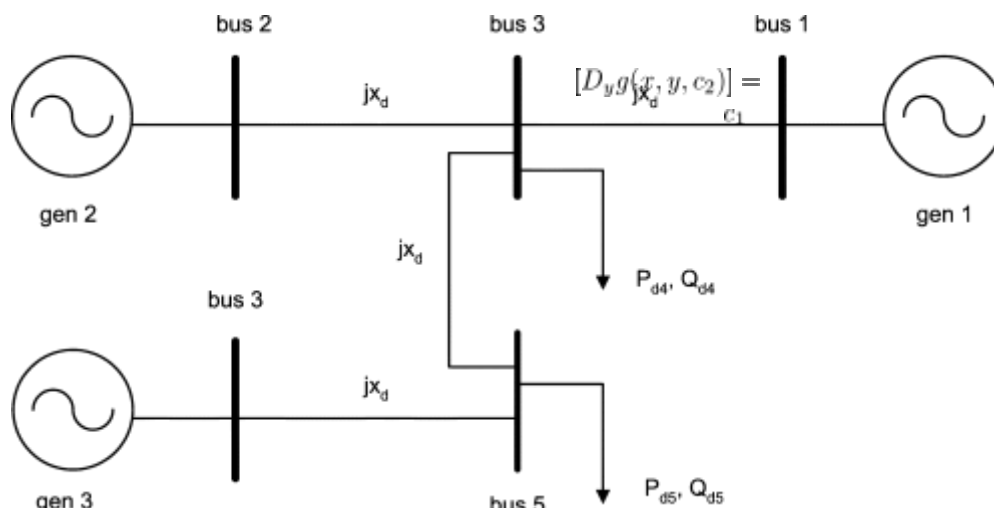


Fig.5. Five-bussystem with three generators and two load buses.

bifurcation is observed at parameters $c_1 = \pm c_2$ for which two equilibrium points, EP_1 and EP_2 , meet at $(\pm c_2, 0)$, which is an SN bifurcation. Finally, beyond the parameter $c_1 = 0$, the DAE of (2.16) does not have any equilibrium. The occurrence of SN and SI bifurcations with the qualitative changes in the number of system equilibria as a function of c_1 is also summarized in Fig. 4.

The singular set of (2.16) separates the constraint manifold into two regions that are connected through the singular points $(-c_2, 0)$ and $(c_2, 0)$. These two regions, which are the half circles in Fig. 3, are defined as follows:

$$C_0 = \{(x, y) \mid -c_2 < x < c_2, y = 0\} \quad (2.17)$$

$$C_1 = \{(x, y) \mid -c_2 < x < c_2, y = \sqrt{c_2^2 - x^2}\}$$

$$C_2 = \{(x, y) \mid -c_2 < x < c_2, y = -\sqrt{c_2^2 - x^2}\}$$

(2.18)

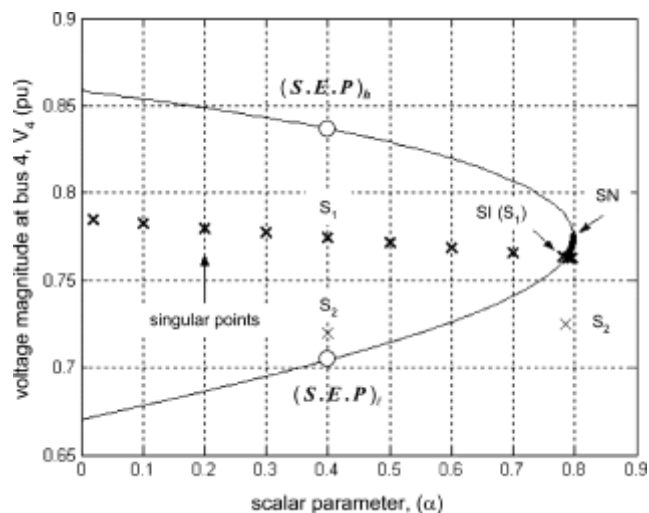


Fig.6. Voltage magnitude at bus 4 (V) and singular points versus parameter

Within the region, C_0 or C_1 , the DAE example of (2.16) could be reduced to the locally equivalent ODEs given below, and the dynamics of the DAE is uniquely determined by the corresponding ODE in each region

$$\dot{x} = -x + \sqrt{c_2^2 - x^2} + c_1 \text{ on } C_0$$

$$(2.19) \dot{x} = -x - \sqrt{c_2^2 - x^2} + c_1 \text{ on } C_1.$$

This example illustrates that even a simple DAE model may exhibit local bifurcations. In the next example, we study bifurcations and singularities of a DAE model of a 5-bus power system and illustrate the application of the lemma for locating SI bifurcation points presented in Section II-B.

Example II: We now present a 5-bus power system example to study bifurcations and demonstrate the application of the lemma for identifying SI bifurcations. The 5-bus system, whose one-line diagram is shown in Fig. 5, has three generators and two constant PQ load buses [13]. The base case bus injections in per unit (pu) with a 100-MW base are as follows:

$$P = [-10, \quad [P_4 \ P_5]^T =$$

$$\text{and } Q = [0, \quad -2]^T$$

Generators, which are undamped, have the internal voltages $E = [1.2]^T$ pu and their terminal voltages are equal to terminal voltages $V_t = \alpha$.

Since the reactance 0.1 pu includes the transient reactances of the generator and transmission line. Generator 1 is chosen as the swing bus with zero angle and all the other phase angles are relative to the swing bus. In order to determine a set of equilibrium points including the SI bifurcation, we

vary mechanical input to the generators 2 and 3 (P_2 and P_3); and real/reactive power demand at bus 4. The resulting search direction in the bus injection space is as follows:

$$dP_g = [0.50 \ 5]^T$$

$$dP_l = [0.50]^T$$

$$dQ_l = [-0.150]^T.$$

Fig. 6 illustrates how the equilibria for the voltage magnitude at bus 4 and their corresponding stability characteristics change with parameter variations. Observe that as the parameter varies, the system equilibria undergo SI and SN bifurcations labeled as SI, SN. As the bus injections are increased through the scalar parameter, both the high-voltage equilibrium and low-voltage equilibrium are dynamically stable. However, at low-voltage equilibrium point undergoes a stability exchange (stable/unstable) due to an SI

$$x_d =$$

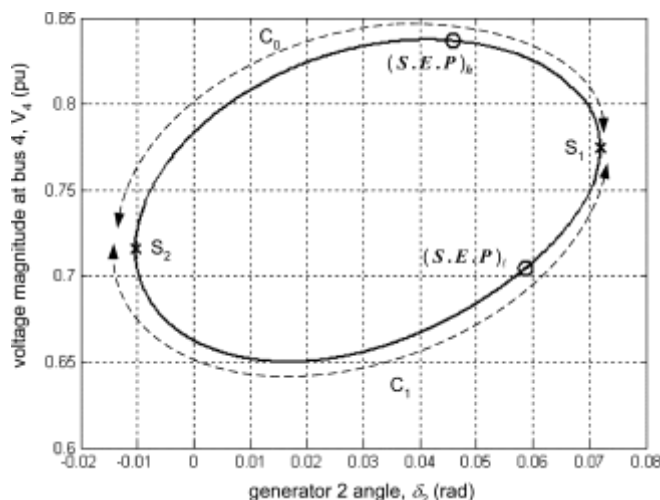


Fig.7.Critical eigenvalues of the system matrix A as the parameter α varies indicating the SI and SN bifurcations.

bifurcation and it becomes a type-1 UEP. Further increase in the parameter causes the high- and low-voltage equilibrium to meet at an SN bifurcation for $\alpha = 0.8$.

The SN and SI bifurcations are detected by monitoring the eigenvalues of system matrix (2.10) as the system moves from one equilibrium point to another with changes in the bifurcation parameters.

Fig.7 shows how two critical eigenvalues of the system matrix move as α changes from 0.773 to 0.8 along the lower branch of nose curve; which lead to SI and SN bifurcations. The arrows indicate the direction of increase in the parameter. Just before the SI bifurcation; say at $\alpha = 0.773$, one of the critical eigenvalues (please note that non-critical ones are not shown in Fig.7) are located in the left half plane, which implies stability. As the parameter change from 0.773 to 0.8, one of the complex eigenvalue moves (in jump fashion) to the right half plane and becomes a large positive number while the other eigenvalue stays in the left half plane but it becomes a large negative real number. Therefore, stability feature of the equilibria undergoes an instantaneous change from stable to unstable with exactly one eigenvalue. This stability exchange is due to an SI bifurcation at which the Jacobian matrix has a simple eigenvalue at the origin and one of the eigenvalues of system matrix becomes unbounded [7]. A clear picture of the occurrence of the SI bifurcation with a much larger real eigenvalue can be obtained at the expense of simulation time [18]. As α increases further, an SN bifurcation occurs at $\alpha = 0.8$ and one of the critical eigenvalues becomes zero while the other one remains in the left half plane. The SN bifurcation corresponds to the point of maximum loading for this particular load increase pattern of the DAE system.

Fig.6 also shows singular points at various values of α along the nose curve, which are depicted by (x) and labeled as S_1 and S_2 . In Section III, we will present a method to compute these singular points. It is worth mentioning here that there are multiple singular points at any given parameter. However, we are interested in those that eventually meet with one of the equilibria located in the lower branch of the nose curve as the parameter is subject to vary as illustrated in Fig.6. Note that the singular points S_1 and S_2 are located in the left half plane.

0.773. The critical eigenvalues (please note that non-critical ones are not shown in Fig.7) are located in the left half plane, which implies stability. As the parameter change from 0.773 to 0.8, one of the complex eigenvalue moves (in jump fashion) to the right half plane and becomes a large positive number while the other eigenvalue stays in the left half plane but it becomes a large negative real number. Therefore, stability feature of the equilibria undergoes an instantaneous change from stable to unstable with exactly one eigenvalue. This stability exchange is due to an SI bifurcation at which the Jacobian matrix has a simple eigenvalue at the origin and one of the eigenvalues of system matrix becomes unbounded [7]. A clear picture of the occurrence of the SI bifurcation with a much larger real eigenvalue can be obtained at the expense of simulation time [18]. As α increases further, an SN bifurcation occurs at $\alpha = 0.8$ and one of the critical eigenvalues becomes zero while the other one remains in the left half plane. The SN bifurcation corresponds to the point of maximum loading for this particular load increase pattern of the DAE system.

Fig.6 also shows singular points at various values of α along the nose curve, which are depicted by (x) and labeled as S_1 and S_2 . In Section III, we will present a method to compute these singular points. It is worth mentioning here that there are multiple singular points at any given parameter. However, we are interested in those that eventually meet with one of the equilibria located in the lower branch of the nose curve as the parameter is subject to vary as illustrated in Fig.6. Note that the singular points S_1 and S_2 are located in the left half plane.

Fig.6 also shows singular points at various values of α along the nose curve, which are depicted by (x) and labeled as S_1 and S_2 . In Section III, we will present a method to compute these singular points. It is worth mentioning here that there are multiple singular points at any given parameter. However, we are interested in those that eventually meet with one of the equilibria located in the lower branch of the nose curve as the parameter is subject to vary as illustrated in Fig.6. Note that the singular points S_1 and S_2 are located in the left half plane.

Fig.6 also shows singular points at various values of α along the nose curve, which are depicted by (x) and labeled as S_1 and S_2 . In Section III, we will present a method to compute these singular points. It is worth mentioning here that there are multiple singular points at any given parameter. However, we are interested in those that eventually meet with one of the equilibria located in the lower branch of the nose curve as the parameter is subject to vary as illustrated in Fig.6. Note that the singular points S_1 and S_2 are located in the left half plane.

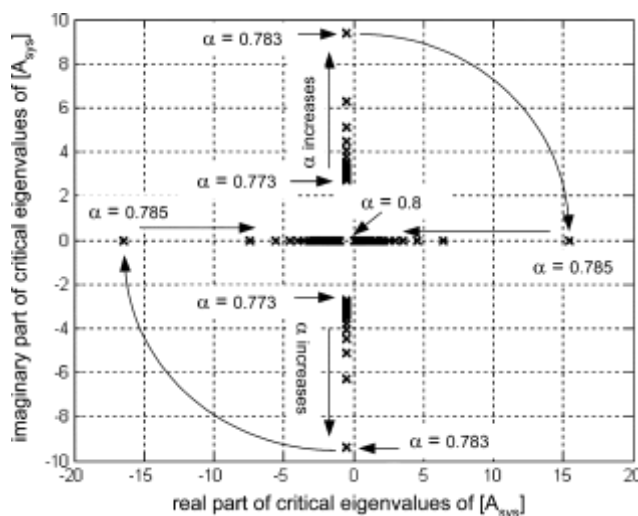


Fig.8.Constraint manifold projection onto the $(V_4; \delta_2)$ -space at $\alpha = 0.4$.

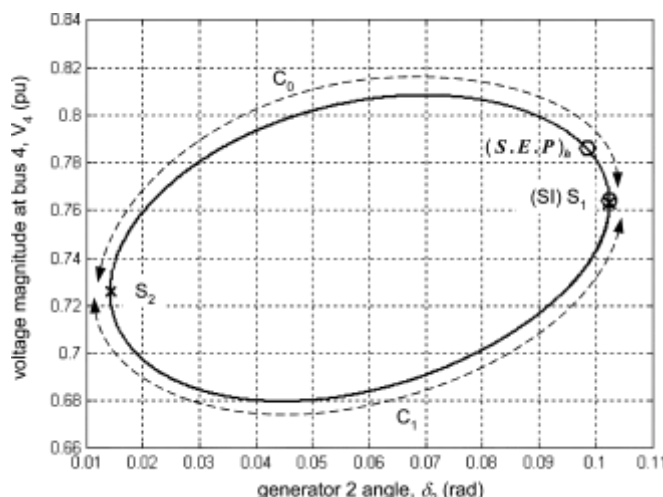


Fig.9.Constraint manifold projection onto the $(V_4; \delta_2)$ -space at $\alpha = 0.785$

illustrating the occurrence of a SI bifurcation.

point S_1 at $\alpha = 0.785$ coincides with low-voltage equilibrium indicating a SI bifurcation. In Fig. 6, we also depict another singular point S_2 for $\alpha = 0.4$ and clearly show the relative locations of other singular points that are not associated with the SI bifurcation. The relative location of singular points with respect to equilibria and SI bifurcation point can be clearly seen using 2-D projections of the constraint manifold. Fig. 8 shows a 2-D projection of the constraint manifold onto the $(V_4; \delta_2)$ -space for $\alpha = 0.4$.

The constraint manifold consists of two voltage causal regions (C_0 and C_1) separated by singular points S_1 and S_2 . Note that each voltage causal region contains dynamically stable equilibrium points (SEPs) labeled as SEP_h and SEP_t . These equilibrium points correspond to high- and low-voltage equilibrium points as shown in Fig. 6. Singular points S_1 and S_2 are the

same as S_1 and S_2 shown in Fig. 6 at $\alpha_{SI} = 0.785$ and they indicate the bifurcations of the algebraic variables (i.e., load bus voltage magnitudes and angles) when generator angles are considered as parameters. It will be informative to illustrate the occurrence of the SI bifurcation by using the constraint manifold projection. Fig. 9 shows the same 2-D projection onto the $(V_4; \delta_2)$ -space for $\alpha = 0.4$. This time, however, the low-voltage equilibrium point SEP_t (V_4, δ_2)

$\alpha = 0.4$

SEP_h SEP_t

moves along the region C_1 as $-\beta_{t0}$ increases from 0.785 to and coincides with the singular point S_1 while the high voltage bus e_1 stays in the region C_0 . Note that for this load increase pattern, both equilibria move toward the singular point S_1 not toward S_2 along the regions as the parameter varies. Therefore, S_2 or any other singular points rather than S_1 are not associated with the SI bifurcation. We now illustrate the application of the lemma to this power-system example. According to the lemma, recall that we can find a new set of bus injections such that any of the singular points along the nose curve shown in Fig. 6 can be an SI bifurcation point. For illustrative purposes, we choose the singular point S_1 at $\beta_{t0} = 0.785$. For the 5-bus system, the vectors of β_g and contain net power injections at the buses. Specifically, $P_g = [P_1, P_2, P_3, P_4, P_5]^T$ and $Q_{st} = [Q_1, Q_2, Q_3, Q_4, Q_5]^T$ where P_g and Q_{st} are in pu.

At the parameter $\beta_{t0} = 0.785$, the bus injection vectors would be $P_g = [-5, 0, 0, 0, 0]^T$ pu and $Q_{st} = [0, 0, 0, 0, 0]^T$ pu. The corresponding mismatch vector at the singular point is $\Delta P_{sg} = [0, 0, 0, 0, 0]^T$ pu. We can adjust the injection of the buses 2 and 3 such that the singular point S_1 will be an SI bifurcation point. The new injection at the generator buses would be $P_g^{new} = [0, 5.115, 5.541, 0, 0]^T$ pu. Note that injections at the load buses (buses 4 and 5) remain unchanged and the corresponding swing bus injection is P_1 pu obtained by $P_1 = -P_2 - P_3 - P_4 - P_5$.

After having illustrated local bifurcations and singularities of the relatively simple DAEs, we are now at a stage of presenting methods for computing them. In Section III, we first briefly summarize a commonly used algorithm to compute equilibrium points and their associated bifurcations, and then we present a search method for computing singular points at any given parameter along the nose curve.

III. IDENTIFICATION OF EQUILIBRIUM AND SINGULAR POINTS

A. Identification of System Equilibria
 In this section, we summarize the method implemented in VST for computing equilibria and their associated static bifurcations as the parameter varies. The starting point for the bifurcation analysis of the power-system model (2.2) is the identification of system equilibria. For a given set of parameters β_0 , an equilibrium point satisfies two algebraic equations

$$f(x_0, y_0) = 0, g(x_0, y_0) = 0 \quad (3.1)$$

Load flow analysis is basically the identification of the set of equilibrium points of (3.1). The VST implements load flow calculations that function up to the point of collapse (SN bifurcation point). Conventional numerical methods for computing equilibria, such as the NR method, must be modified in order to obtain reliable results near bifurcation points. Two methods have been applied to power-system analysis: the continuation (or homotopy) [29] method and the direct (or point of collapse) method [30]. The direct method proposed by Seydel to compute the branch points in single-parameter nonlinear algebraic equations has proved remarkably effective in power-system applications. Many investigators have implemented variants of this approach, imaginatively tailored to the special features and requirements of power systems [31]–[34]. We refer to these as a group as the NRS method. We describe our implementation of the Seydel's direct method. For convenience, we collect the dependent variables into a single vector which we denote by (i.e.,

$z = [x^T, y^T, \alpha]^T$). Similarly, we collect the pair of functions f and g into the single function $F(z, \alpha) = [f^T, g^T]^T$. Note that the vector of parameters $\alpha = [\beta_g, \beta_{t0}]^T$ is replaced by the scalar bifurcation parameter that parameterizes through (2.14). We seek to investigate the zeros of $F \in \mathbb{R}^N$ (equilibria) as a function of the bifurcation parameter α where

$$F(z, \alpha) = 0 \quad (3.2)$$

The standard NR method applied to (3.2) is

$$z_{i+1} = z_i + \Delta z_i \quad (3.3)$$

where Δz_i is the load flow Jacobian matrix $J = [D_z F]$. However, the NR method breaks down near (static) bifurcation points, i.e., when $\det(J) = 0$. In generic one-parameter families the dimension of a bifurcation point is precisely one, i.e.,

Thus, to locate such a point we seek values for α and nontrivial $v \in \mathbb{R}^N$ which satisfy

$$F(z, \alpha) = 0, \quad [D_z F(z_i, \alpha)]v = 0, \quad w^T [D_z F(z_i, \alpha)] = 0 \quad (3.4a)$$

The requirement for nontriviality of v may be stated by $\|v\| > 0$ or $\|w\| > 0$ (3.4c)

One basic approach to finding bifurcation points is to apply the NR method to (3.4). This is the NRS method. Data that satisfies (3.4) will be denoted as (z_b, α_b) , and we designate the Jacobian J_b . Note that the vector $[D_z F(z_b, \alpha_b)]$

has special significance. They are, respectively, the right and left eigenvectors corresponding to the zero eigenvalue of J_b . The eigenvector spans the kernel of J_b and spans the kernel of J_b^T . Once a bifurcation point is located, it is feasible to modify the above method to compute points around the old (nose) of the equilibrium surface

$$(3.5) \quad \text{for values of } [-\varepsilon_1, \varepsilon_2] \text{ with } \varepsilon_1, \varepsilon_2 > 0$$

This allows computation of equilibrium points close to the bi-furcation point where the conventional NR calculations $\lambda = 0$ would fail. Of course, these points correspond to the SN bifurcation point. The above method can be effective but it has the disadvantage that it is significantly more computationally intensive than a standard load flow. It involves solving F equations as opposed to, and it requires computing second-order derivatives of F . However, it is possible to devise potentially more efficient

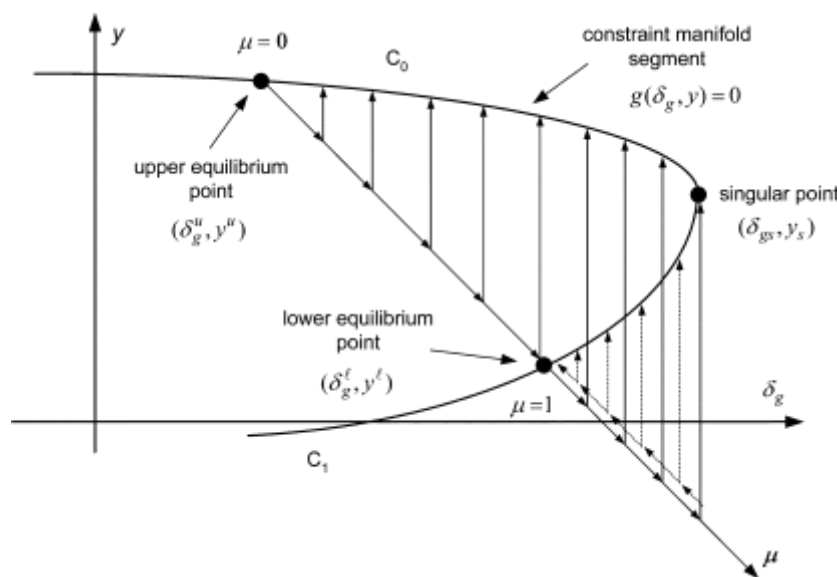


Fig.10. Graphical illustration of the method for computing singular points.

methods that exploit the fact that (3.4b) and (3.4c) are linear in μ and [33].

In VST, governing equations of the classical model and Jacobian matrix including the second derivatives have been constructed symbolically and a three-stage load flow method, has been implemented to compute equilibria and bifurcations. First, the standard NR method is used until it fails to converge. Then, it automatically switches to the NRS method to find load flow solutions at and around SN bifurcation point. After passing through the SN bifurcation point, the standard NR method is switched back to compute low-voltage solutions.

B. Identification of Singular Points

In this section, we present an algorithm to compute singular points of the DAE model of (2.2) at any given parameter value along the nose curve. The method is an iterative technique that combines well-known NR and NRS methods, which are commonly used to compute SN bifurcations in power system

as explained in Section III-

A. The proposed algorithm benefits from the knowledge of the system equilibria and the occurrence of the SI bifurcation. Generator angles are parameterized through a scalar parameter in the constraint manifold. Then, at any given parameter value, the identification of a singular point is formulated as a bifurcation problem of a set of algebraic equations whose parameters are the generator angles. In the following, we explain why we parameterize generator angles and how this parameterization is achieved.

1) Parameterization of Generator Angles: Recall that the algebraic part of the DAE model of (2.2) represents the real and reactive power equations at the PQ load buses $g(\delta_g, y)$ (3.6)

At a fixed parameter value, the constraint manifold consists of a set of points (δ_g, y) satisfying (3.6). As explained and illustrated in Section II (see Figs. 8 and 9 of Example II) the constraint manifold contains voltage causal regions and singular points

connecting them. Fig. 10 hypothetically illustrates a magnified segment of the constraint manifold composed of two voltage causal regions, C_0 and C_1 , and a singular point (δ_{gs}, y_s) . Note that the region C_0 contains the upper equilibrium point while the region C_1 contains the lower equilibrium point. These equilibria correspond to the high- and low-voltage solutions at a given parameter value along the nose curve (see Fig. 6 for an example), which are known to us from the computation of equilibria and bifurcations explained in Section III-A.

Observe that for any given generator angle δ_g , there are two corresponding solutions for the algebraic variables that represent the load bus voltage magnitude and phase angle. As the generator angle increases, these two solutions move along the regions C_0 and C_1 until they meet at the singular point.

At the singular point, the Jacobian matrix becomes singular and there is no solution for it if further increased. This observation indicates that algebraic variables show a nose curve type of behavior as the generator angles vary, and they undergo an SN bifurcation at the singular point. This behavior is similar to the SN bifurcation of the equilibria as the bus injections change. This observation leads us to use generator angles as parameters and to seek methods to compute the SN bifurcations of algebraic variables, which is a singular point of the DAE model.

A recent work by Singh and Hiskens [16] on the characterization of the stability boundary of the DAE model has illustrated the fact that singular surfaces lie on the boundary of the stability region of a SEP and they contain infinitely many singular points. However, as illustrated in Figs. 6–9 of Section II, we are only interested in computing those singular points that eventually intersect with an SI bifurcation point for a given bus injection pattern. Specifically, we also assume that we specify a priori which injections will change to create other singular points.

In order to trace the corresponding segment of the manifold and to compute the singular points shown in Fig. 10, we need to implement an iterative method that initiates at a point in C_0

and ends up at another point in C_1

passing through the singular point (δ_{gs}, y_s) . The upper and lower equilibrium points are the obvious choice for the starting and ending points of the algorithm since they are available to us from the equilibria computation. The following parameterization of the generator angles will achieve that purpose:

$$\delta_g \quad (3.7)$$

where δ_g^u and δ_g^l are (nl) -dimensional vectors representing the generator angles at the upper and lower equilibrium points at a given parameter value y (or equivalently by (2.14)), respectively, and is a new scalar bifurcation parameter. With this parameterization, the identification of the singular point of the constraint manifold at a fixed parameter reduces to a single parameter bifurcation problem of the following equation:

$$(3.8)$$

Note that we drop the parameter β in (3.8) for the sake of simplicity in the notation. Clearly, the SN bifurcation of the algebraic variables as the bifurcation parameter changes would be a singular point of the constraint manifold at the corresponding parameter. In Section III-B-2, we describe a two-staged algorithm that implements the NR and NRS methods to locate the singular points. A similar method has also been reported in [16] to compute the singular point on the impasse surface that has the minimum potential energy as to characterize the stability boundary for the case when the boundary does not contain any unstable equilibria and/or periodic orbits.

2) Combined NR and NRS Method: As we have explained in Section III-B-I, a singular point of the DAE model at a given parameter is a static bifurcation point of the load bus voltage magnitude and phase angles when the generator angles are subject to vary. Thus, the problem of computing a singular point is equivalent to identification of the SN bifurcation of the algebraic (3.8) as the scalar parameter varies [thus, change through (3.7)]. Therefore, we seek a singular point in the constraint manifold such that

In other words, the singular points must belong to the constraint manifold and the Jacobian matrix must have a simple eigenvalue at the origin. We can rewrite these two conditions as follows:

$$(3.9)$$

$$(3.10)$$

$$\|v_y\|_2 \neq 0 \quad (3.11)$$

where

y is the algebraic variables (load bus voltage magnitude and phase angles), J is the Jacobian matrix of the algebraic equations, v_y is the right eigenvector corresponding to the zero eigenvalue of the Jacobian matrix, and

μ is the bifurcation parameter used to vary the generator angles. Observe that (3.11) assures that the eigenvector is nontrivial. Equation (3.10) together with

(3.11) establishes the singularity of Jacobian matrix.

The conventional NR method is the most common iterative technique to compute the roots of nonlinear algebraic

equations. This method can be applied to (3.8) as follows:

$$(3.12)$$

The above

iterative scheme works well almost everywhere in the constraint manifold. However, it will fail to converge around singular points since the Jacobian matrix is close to singularity. The NRS method has been effectively used to compute static bifurcation points in power systems. In order to apply the NRS method to (3.9)–(3.11), are an eigenvalue of A is introduced as an independent variable. That will make it possible to implement an iterative scheme that goes around the singular point

$$h_2 = [D_y g(y, \mu) - \lambda I] v_y = 0$$

$$h_3 \|v_y\|_2 - 1 = 0 \quad (3.13)$$

There are a total of

$2m + 1$ in (3.13) and the same number of unknown variables while λ is the independent variable. For a given (y, μ) , (3.13) can be solved for the unknowns

$$\hat{z} = [y \quad v_y$$

$$\lambda]^T \quad (3.14)$$

where $[h_2^T \ h_3^T]^T$ and v_y is the corresponding extended Jacobian matrix of (3.13).

The NRS algorithm, like any other Newton-iterative method, needs a good initial condition, that is a point in the constraint manifold close enough to the singular point along with the smallest real eigenvalue of

A and the corresponding right eigenvector.

Otherwise, we may experience convergence problems. Therefore, we first use the NR method. The NR computations proceed starting at the upper equilibrium point (0)

along the constraint manifold until it fails to converge.

The last successful NR data point is used to implement an inverse iteration method [35] for estimating the eigenvalue of A nearest λ_0 , and the corresponding right eigenvector. These data are then used to initiate an NRS procedure using (3.14) to compute around the singular point for values of $[\lambda - \epsilon_1, \epsilon_2]$ with $\epsilon_1, \epsilon_2 > 0$. The value

is always included and data at the singular point is there by

obtained.

In order to compute singular points at various parameters along the nose curve and depict them together with the equilibria in a 2-D nose curve, the following procedure, which is also graphically illustrated in Fig. 11, is implemented in VST.

Step 1) Choose a load (bus injections) increase pattern. Step 2) Compute equilibrium points (nose curve), the sta-

bility properties of the equilibria and locate local bifurcations. Step 3) Choose a parameter μ along the nose curve and fix it.

Step 4) Compute the singular point at this parameter.

Step 5) Repeat the steps 3–4 as many times as desired up to the parameter μ_2 .

Step 6) Depict singular points in the nose curve.

$$[D_y g(y, \mu)]$$

$$h_1 = g(y, \mu) = 0$$

$$= 0.$$

$$(2m + 1)$$

$$\lambda$$

$$\lambda$$

$$\mu]^T$$

$$[D_z H(\hat{z}_i)] \Delta \hat{z} = -H(\hat{z}_i), \quad \hat{z}_{i+1} = \hat{z}_i + \Delta \hat{z}$$

$$H = [h_1^T \quad [D_z H(\hat{z})]$$

$$[D_y g(y, \mu)]$$

$$v_y$$

$$(\mu =$$

$$[D_y g(y, \mu)] \quad \lambda = 0$$

$$v_y$$

$$\lambda \in \quad \epsilon_1, \epsilon_2 > 0$$

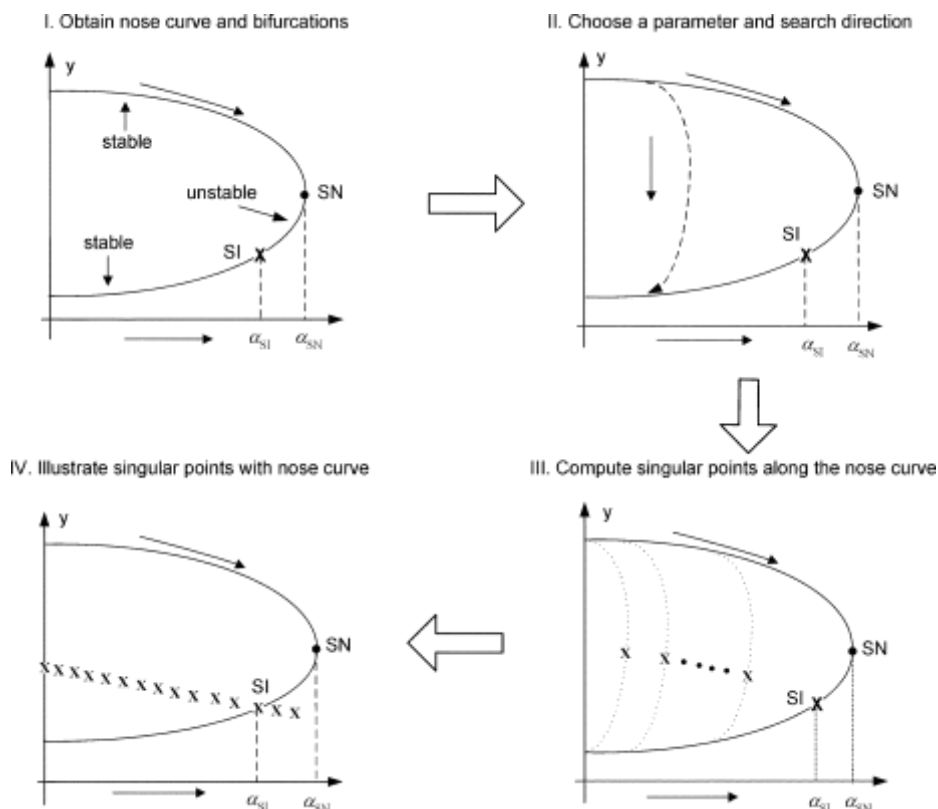


Fig. 11. Graphical illustration of the procedure for computing singular points and depicting them along the nose curve.

In Section IV, we will illustrate the application of our method that includes the steps given above to the IEEE 118-bus system.

IV. SIMULATION RESULTS

In this section, we present results on the SI bifurcation and singular points for the IEEE 118-bus test system. The real and reactive powers at bus 75 have been increased according to (2.14). Fig. 12 illustrates how the voltage magnitude at bus 75 changes with parameter variations. As can be seen, two kinds of bifurcations are identified, namely SN and SI bifurcations. As the parameter increases both upper and lower parts of the nose curve are dynamically stable. At

the system undergoes a stability exchange associated with the SI bifurcation and the stability feature of the lower equilibrium points changes qualitatively, from stable to unstable. As the parameter further increases, one stable (upper part) and one type-1 unstable (lower part) equilibrium point meet at an SN bifurcation point for which is the tip of the nose curve. Beyond the SN bifurcation point, there is no feasible solution to the load flow equations. The stability properties of the lower part of the nose curve are certainly model dep

endent. When the load dynamics are included the entire lower part of the nose curve might be unstable. Fig. 12 also depicts singular points at different parameter values. The parameter value is especially important in the sense that it enables us to check whether the singular point search method gives correct results. Recall that at the SI bifurcation occurs and all the state information at this parameter value is available to us from equilibrium

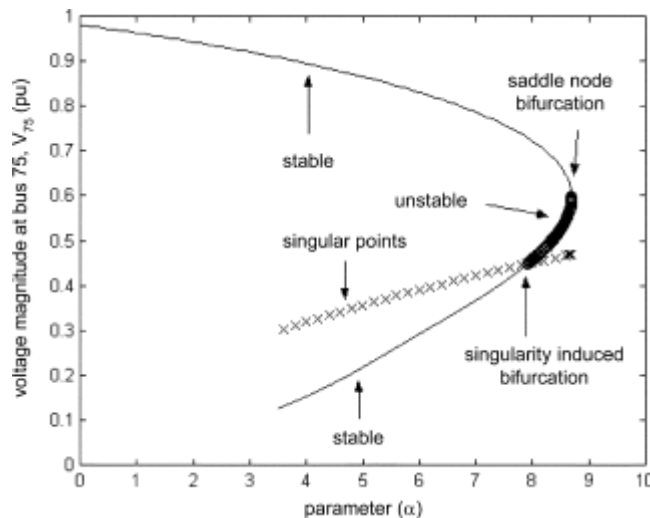


Fig. 12. Voltage magnitude at bus 75 versus parameter alpha (α) with singular points when the real and reactive power at bus 75 increase.

and bifurcation analysis. The SI bifurcation point also belongs to the singular set defined by (2.9). It is expected that the proposed method should give the same result as that of the bifurcation analysis.

As seen from Fig. 12, this is indeed the case. Observe that for the voltage magnitude at bus 75

singular points at each parameter value lies between the higher and lower voltage solutions until the SI occurs. Note that the lower part of the nose curve may not be practical operating points due to the low-voltage profile. However, this is not the general case as shown in Fig. 13 that depicts the voltage magnitude at bus 63

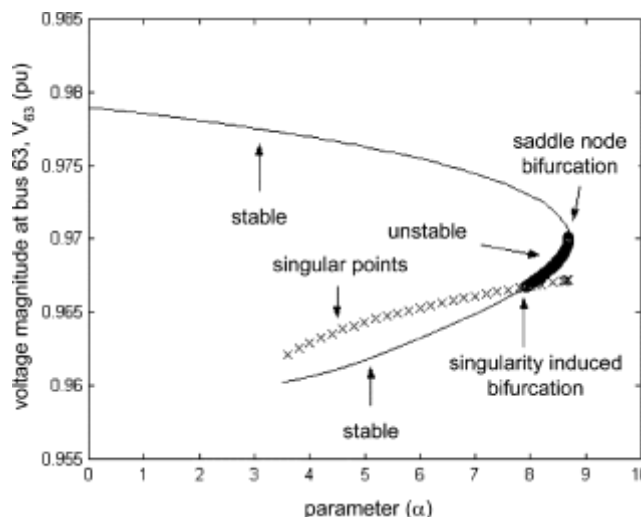


Fig. 13. Voltage magnitude at bus 63 versus parameter alpha (α) with singular points when the real and reactive power at bus 75 increase.

for the same load increase pattern. The lower part of the nose curve and singular points including the SI bifurcation point lie above 0.95 pu, which is usually considered to be the low-voltage threshold value for normal operation of the po-

wers systems.

V. CONCLUSION AND FUTURE WORK

In this paper, we have presented an

iterative method to locate and identify singular points of the DAE model of power system. In the method, we use generator angle to parameterize the algebraic part of the DAE model and we identify the singular points as being the SN bifurcation of the algebraic part of the DAE model. We have shown by a lemma that any singular point at a given set of bus injections is an SI bifurcation point at another set of bus injections. We have combined static information from the SN and dynamic information from the singular point together in order to provide a comprehensive picture of the system stability. We have updated the VST to include singular point computations. Simulation results on a 5-bus system and the IEEE 118-bus system have been presented. We have illustrated singular points with the traditional nose curve for different load change scenarios.

As future work, an energy function approach should be implemented in order to provide a dynamic security index that considers the singular points. Specifically, the dynamic stability margin of a given operating point could be computed as the energy difference between the current operating point and the singular point. This scalar energy value would be the dynamic security index. Moreover, in order to complete the picture as a static security index as being the energy difference between the current operating point and the point of collapse should be combined with the dynamic security index.

REFERENCES

- [1] Voltage stability assessment, procedures, and guides (IEEE/PES Power system stability subcommittee special publication), IEEE/PES. (2001, Jan.). [Online]. Available: <http://www.power.uwaterloo.ca>.
- [2] H. G. Kwatny, A. K. Pasrija, and L. Y. Bahar, "Static bifurcations in electric power networks: Loss of steady state stability and voltage collapse," *IEEE Trans. Circuits Syst. I*, vol. 33, no. 10, pp. 981–991, Oct. 1986.
- [3] M. A. Pai, P. W. Sauer, and B. Lesieutre, "Static and dynamic nonlinear loads and structural stability in power systems," *Proc. IEEE*, vol. 83, pp. 1562–1572, Nov. 1995.
- [4] C. A. Cañizares, "On bifurcations, voltage collapse and load modeling," *IEEE Trans. Power Syst.*, vol. 10, pp. 512–522, Feb. 1994.
- [5] H. G. Kwatny, R. F. Fischl, and C. O. Nwankpa, "Local bifurcation in power systems: Theory, computation, and application," *Proc. IEEE*, vol. 83, pp. 1456–1483, Nov. 1995.
- [6] B. Lee and V. Ajjarapu, "A piecewise global small-disturbance voltage-stability analysis of structure-preserving power-system models," *IEEE Trans. Power Syst.*, vol. 10, pp. 1963–1971, Nov. 1995.
- [7] V. Venkatasubramanian, H. Schättler, and J. Zaborszky, "Local bifurcations and feasibility regions in differential-algebraic systems," *IEEE Trans. Automat. Contr.*, vol. 40, pp. 1992–2013, Dec. 1995.
- [8] —, "Global voltage dynamics: Study of a generator with voltage control, transmission and matched MW load," *IEEE Trans. Automat. Contr.*, vol. 37, pp. 1717–1733, Nov. 1992.
- [9] Y. Lijun and T. Yun, "An improved version of the singularity-induced bifurcation theorem," *IEEE Trans. Automat. Contr.*, vol. 46, pp. 1483–1486, Sept. 2001.
- [10] R. E. Beardmore, "Stability and bifurcation properties of index-1 DAEs," *Numer. Algor.*, vol. 19, pp. 43–53, 1998.
- [11] R. Riaza, S. L. Campell, and W. Marszalek, "On singular equilibria of index-1 DAEs," *Circuits Syst. Signal Process*, vol. 19, no. 2, pp. 131–157, 2000.
- [12] C. L. DeMarco and A. R. Bergen, "Applications of singular perturbation techniques to power-system transient stability analysis," in *Proc. IEEE Int. Symp. Circuits Systems*, 1984, pp. 597–601.
- [13] K. L. Praprost and K. A. Loparo, "An energy function method for determining voltage collapse during a power-system transient," *IEEE Trans. Circuits Syst. I*, vol. 41, pp. 635–651, Oct. 1994.
- [14] I. A. Hiskens and D. J. Hill, "Energy function, transient stability and voltage behavior in power systems with nonlinear loads," *IEEE Trans. Power Syst.*, vol. 4, pp. 1525–1533, Oct. 1989.
- [15] —, "Failure modes of a collapsing power system," in *Proc. Bulk Power System Voltage Phenomena II—Voltage Stability and Security*, Deep Creek Lake, MD, Aug. 1991, pp. 53–63.
- [16] C. Singh and I. A. Hiskens, "Direct assessment of transient singularity in differential-algebraic systems," in *Proc. 2001 IEEE Int. Symp. Circuits and Systems (ISCAS'01)*, Sydney, Australia, May 06–09, 2001, pp. III/201–III/204.
- [17] C. Singh, "Direct assessment of transient viability in power systems

- with dynamic loads," Ph.D. dissertation, Univ. of Newcastle, Newcastle, Australia, 2001.
- [18] S. Ayasun, C. O. Nwankpa, and H. G. Kwatny, "Bifurcation and singularity analysis with voltage stability toolbox," in Proc. 31st North American Power Symp. (NAPS), San Luis Obispo, CA, Oct. 1999, pp.390–397.
- [19] —, "Parameter space depiction of the stability limits in the presence of singularities," in Proc. 2001 IEEE Int. Symp. Circuits and Systems (ISCAS'01), Sydney, Australia, May 06–09, 2001, pp.III/125–III/128.
- [20] W. M. Boothby, *An Introduction to Differentiable Manifolds and Riemannian Geometry*. San Diego, CA: Academic, 1986.
- [21] J. Guckenheimer and P. Holmes, *Nonlinear Oscillations, Dynamical Systems and Bifurcations of Vector Fields*. New York: Springer-Verlag, 1983.
- [22] R. Seydel, *Practical Bifurcation and Stability Analysis-From Equilibrium to Chaos*. New York: Springer-Verlag, 1994, vol. 5.
- [23] I. Dobson and H.-D. Chiang, "Toward a theory of voltage collapse in electric power systems," *Syst. Contr. Lett.*, vol. 13, pp.253–262, 1989.
- [24] I. Dobson, "Observations on the geometry of saddle node bifurcation and voltage collapse in electrical power systems," *IEEE Trans. Circuits Syst.*, vol. 39, pp.240–243, Mar. 1992.
- [25] K. Kim, H. Schättler, V. Venkatasubramanian, J. Zaborszky, and P. Hirsch, "Methods for calculating oscillations in large power systems," *IEEE Trans. Power Syst.*, vol. 12, pp.1639–1648, Nov. 1997.
- [26] A. A. P. Lerm, C. A. Cañizares, F. A. B. Lemos, and A. S. e Silva, "Multi-parameter bifurcation analysis of power systems," in Proc. North American Power Symp. (NAPS), Cleveland, OH, Oct. 1998, pp.76–82.
- [27] A. Arapostathis, S. S. Sastry, and P. Varaiya, "Global analysis of swing dynamics," *IEEE Trans. Circuits Syst.*, vol. 29, pp.673–679, Oct. 1982.
- [28] G. M. Hung, L. Zhao, and X. Song, "A new bifurcation analysis for power-system dynamic voltage stability studies," in Proc. IEEE PES Winter Meeting, New York, Feb. 2002, pp.882–888